Available online at www.sciencedirect.com
ScienceDirect
Journal of Solid State Chemistry 180 (2007) 654–660
JOURNAL OF SOLID STATE CHEMISTRY
www.elsevier.com/locate/jssc

Carbon nanotube assisted synthesis of CeO_2 nanotubes

Dengsong Zhang[a,b,*], Hongxia Fu[a], Liyi Shi[a,b,*], Jianhui Fang[a], Qiang Li[c]

[a]*Department of Chemistry, Shanghai University, Shanghai 200444, China*
[b]*School of Material Science and Engineering, Shanghai University, Shanghai 200072, China*
[c]*Center of Analysis and Test, Shanghai University, Shanghai 200444, China*

Received 11 August 2006; received in revised form 17 November 2006; accepted 19 November 2006
Available online 23 November 2006

Abstract

CeO_2 nanotubes have been synthesized facilely using carbon nanotubes (CNTs) as templates by a liquid phase deposition method. The properties of the CeO_2 nanotubes were characterized by scanning electron microscopy (SEM), transmission electron microscopy (TEM), X-ray diffraction (XRD), X-ray photoelectron spectrum (XPS) as well as thermogravimetry and differential thermal analysis (TG-DTA). The obtained CeO_2 nanotubes with a polycrystalline face-centered cubic phase have a uniform diameter ranging from 40 to 50 nm. The CeO_2 nanotubes are composed of many tiny interconnected nanocrystallites of about 10 nm in size. The pretreatment of CNTs and calcination temperature were confirmed to be the crucial factors determining the formation of CeO_2 nanotubes. A possible formation mechanism has been suggested to explain the formation of CeO_2 nanotubes.

Keywords: CeO_2 nanotubes; Carbon nanotubes; Template; Liquid phase deposition

1. Introduction

The one-dimensional (1-D) nanostructure has attracted much attention since the discovery of carbon nanotubes (CNTs) [1]. The potential applications of 1-D nanomaterials in the electric devices, sensors, and others have been proposed due to their special physical and chemical properties [2]. Up to now, the nanotubes have attracted enormous technological and scientific interest. In the past several years, many approaches have been applied in synthesizing metal oxide nanotubes, such as ZnO [3], CuO [4], MnO_2 [5], TiO_x [6], PbO_2 [7], SiO_2 [8], InO_2 [9], and GeO_2 [10]. Recently, Sun et al. [11] used CNT template to prepare α-Fe_2O_3 nanotubes by supercritical fluid at high temperature and pressure. However, no reports on the synthesis of metal oxide nanotubes using CNTs as templates under moderate conditions have been published to date.

CeO_2 is a technologically important rare earth material because of its wide applications as fast ion conductors, oxygen storage capacitors, catalysts, UV blockers, and polishing materials [12]. The synthesis of 1-D CeO_2 nanomaterials has been of great interest in recent years. CeO_2 nanorods/nanowires have been synthesized using anodic alumina membranes as templates [13] or using a surfactant as a structure-directing agent [14]. However, few studies have been reported on the fabrication of CeO_2 nanotubes, except that Tang et al. [15] reported to synthesize CeO_2 nanotubes from $Ce(OH)_3$ nanotubes by a hydrothermal method. The previous reported hydrothermal method needs high pressure and temperature. Therefore, the preparation of CeO_2 nanotubes in moderate conditions still remains challenging [15].

Herein, we firstly report the simple and efficient synthesis of CeO_2 nanotubes using CNTs as templates by a liquid phase deposition method.

2. Experimental section

The CNTs used in this work were prepared by the catalytic decomposition of methane [16], and were ~40 nm in diameter and 1–10 μm in length. In a typical synthesis, a given amount of CNTs was first refluxed in a 30% nitric

*Corresponding authors. Fax: +86 21 6613 4852.
E-mail addresses: dengsongzh@163.com (D. Zhang), sly0726@163.com (L. Shi).

0022-4596/$ - see front matter © 2006 Elsevier Inc. All rights reserved.
doi:10.1016/j.jssc.2006.11.025

acid at 140 °C for 24 h, and then the treated CNTs were dispersed in a 0.05 g/mL $Ce(NO_3)_3$ solution with ultrasonic radiation at room temperature for 1 h. With vigorous stirring, a 0.005 g/mL NaOH solution was added slowly into the above-mixed solutions until the pH value was 10. After rinsing repeatedly and drying at 60 °C, the as-synthesized sample was obtained. The final product was obtained by calcination in air at a heating rate of 5 °C/min from room temperature to 500 °C, and the temperature was maintained at 500 °C for 0.5 h.

The morphologies of the products were observed by field emission scanning electron microscopy (SEM, JEOL JSM-6700F) and field emission transmission electron microscopy (TEM, JEOL JEM-2010F), and powdered samples were dispersed in absolute ethanol by ultrasonication for 10 min in a KQ-250B ultrasonic bath. The powder X-ray diffraction (XRD) measurements were performed with a Rigaku D/MAX-RB X-ray diffractometer by using Cu $K\alpha$ (40 kV, 40 mA) radiation and a secondary beam graphite monochromator. The X-ray photoelectron spectrum (XPS) was recorded on a PHI-5000C ESCA system (Perkin Elmer) with Al $K\alpha$ radiation. Thermogravimetry and differential thermal analysis (TG-DTA) of the samples was carried out with a Netzsch STA 409 PG/PC analyzer at a heating rate of 10 °C/min from room temperature to 1000 °C. The zeta potentials of the CNTs were measured at a concentration of 0.05 mg/mL with a Zetasizer 3000HS analyzer (Malvern, UK). The pH values of the CNT solutions were adjusted from 2.0 to 12.0 by adding a 0.05 M hydrochloric acid or sodium hydroxide solution.

3. Results and discussion

3.1. Characteristics of CeO_2 nanotubes

The morphology of the obtained products was observed with SEM. Fig. 1 shows that the obtained products have a 1-D nanostructure with a uniform diameter ranging from 40 to 50 nm corresponding to that of CNT template. Figs. 1(b) and (c) show that the tips of the 1-D nanostructure are open, indicating the hollow structure, which suggests that the structure is nanotube.

Fig. 2 shows the TEM and HRTEM images of CeO_2 nanotubes. The inner diameter of nanotubes is in the range of 15–30 nm, while the outer diameter is from 40 to 50 nm. It is noted that the nanotube is composed of many tiny interconnected grains at various orientations and the average grain size is of ~10 nm. The crystalline nature of the resultant CeO_2 nanotubes can be verified by the selected area electron diffraction (SAED) pattern. Fig. 2(b, inset) shows that the SAED pattern is basically a ring pattern. This ring pattern can be indexed using the face-centered cubic polycrystalline structure of CeO_2. The HRTEM image in Fig. 2(c) shows the clear (111), (200) and (220) lattice fringes of CeO_2 with the interplanar spacing of 0.31, 0.27 and 0.19 nm, respectively. It should be noted that the products were dispersed in absolute ethanol by high-intensity ultrasonication for 1 h, and the tubular structure still remains, indicating that the nanotubes are stable. It can be explained that the CeO_2 nanocrystals become faceted and neighboring crystals fuse together.

The phases of the samples were further examined by XRD. Fig. 3 confirms that the obtained CeO_2 nanotubes are pure phase products with a face-centered cubic structure according to JCPDS 78-0694. No obvious peaks corresponding to cerium nitrate or other cerium oxides were observed in the powder pattern. The mean nanocrystal size of CeO_2 nanoparticles calculated from the half-width of the strongest 1 1 1 diffraction peak is 10.7 nm, corresponding to the observed size (~10 nm, Fig. 2).

The formation of CeO_2 in the nanotubes was further verified by XPS spectrum. The wide spectrum in Fig. 4 reveals the predominant presence of cerium, oxygen, and carbon (mainly from the contaminant carbon). No other heteroelements, including sodium and nitrogen, were observed, which suggests that there are no unreacted precursors in the products. According to the Ce 3d spectrum (Fig. 4(inset)), it is obvious that the cerium mainly exists as the Ce (IV) oxidation state (882.8 eV) [17]. In addition, the O1 s peak centered at 529.6 eV corresponds to the O^{2-} contribution [17]. Thus, the XPS-detected binding energies of Ce 3d and O 1 s are in agreement with those of the standard CeO_2.

3.2. Affecting factors and mechanism of the formation of CeO_2 nanotubes

Fig. 5 shows the TEM images of the samples calcined at various temperatures. The CNTs are first uniformly coated with CeO_2 nanoparticles by deposition from the liquid phase, and few nanoparticles are observed to be free from the surface of CNTs (Fig. 5(a)). After calcination at 450 °C, the size of the nanocrystals increases and at the same time the layers of CNT templates are attenuated gradually (Fig. 5(b)). When the calcination temperature is further increased to 500 °C, the nanocrystals become faceted and neighboring crystals fuse together as a result of the formation of CeO_2 nanotubes (Fig. 5(c)). Higher temperature treatment results in the formation of discrete CeO_2 nanoparticles from the collapse of tubular structure with the growth of the particle size (Fig. 5(d)). It is clear that the suitable calcination temperature is a key factor to the formation of CeO_2 nanotubes.

Fig. 6 shows the XRD patterns of the samples calcined at various temperatures. The XRD pattern of the uncalcined sample confirms that CeO_2/CNT composites are first formed by this method. The feature peak 0 0 2 of CNT template is observed when the temperature is below 500 °C, while it disappears when the temperature is over 500 °C, which further confirms the above TEM analysis (Fig. 5). It should be noted that the feature peaks of CeO_2 become sharp with increasing the temperature, indicating that the size of nanoparticles increases due to the calcinations.

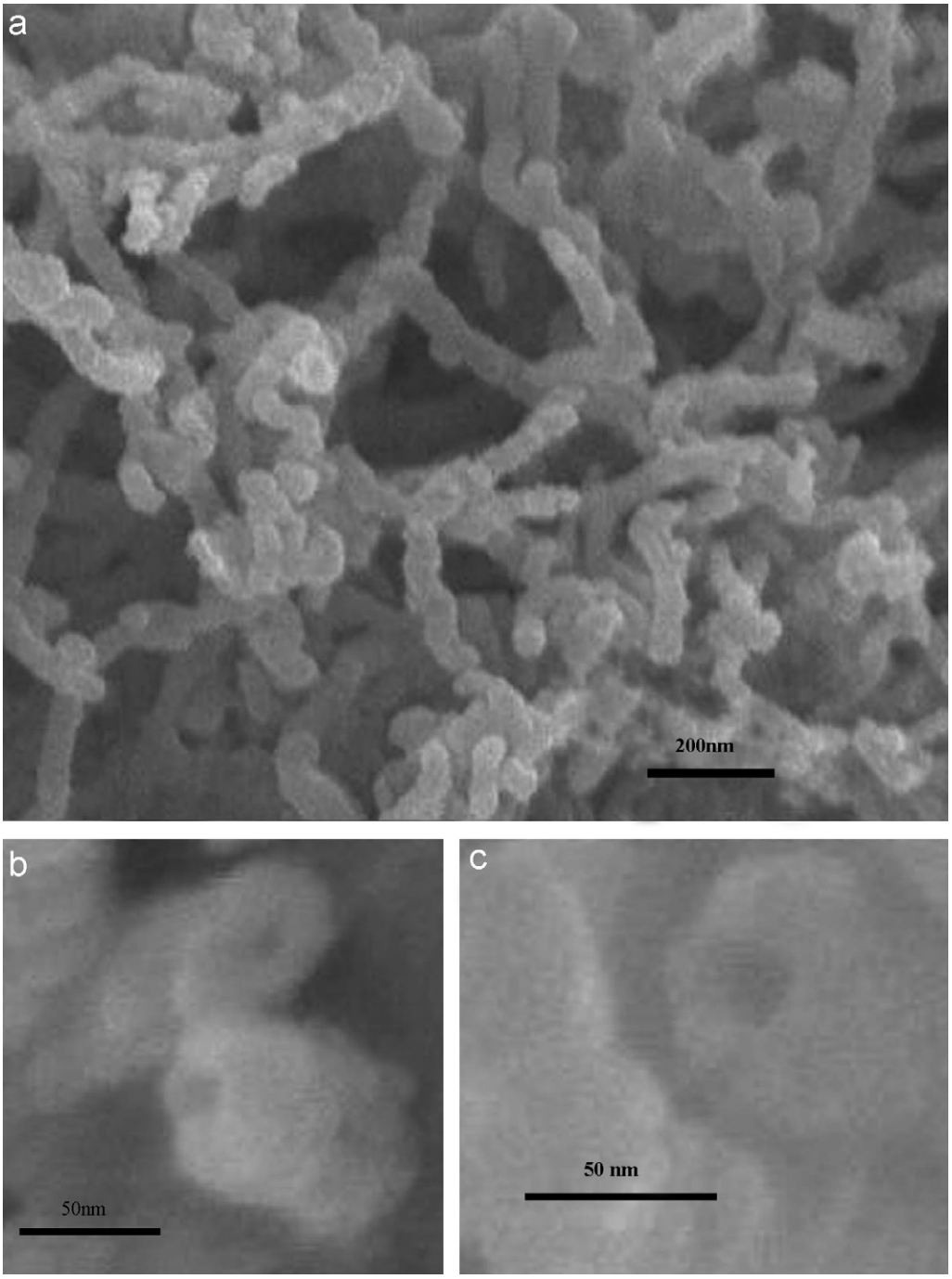

Fig. 1. SEM images of the CeO_2 nanotubes. (a) Overview of SEM image of the CeO_2 nanotubes, (b) SEM image of the tips of CeO_2 nanotubes, and (c) SEM image of the tip of the single nanotube.

According to the above analysis, the XRD-detected features of CeO_2 nanotubes are in agreement with those of the standard CeO_2. Actually, the obtained nanotubes exhibit a light yellow color, similar to the standard CeO_2, while the sample calcined at 450 °C exhibits a slightly grayer color. As the XRD-calculated mean nanocrystal size of CeO_2 calcined at 450 and 500 °C changes slightly (10.2 and 10.7 nm, respectively), it can be concluded by the color that the CNT template still exists at 450 °C while disappears at 500 °C. Fig. 7 shows the TG-DTA curves of the CeO_2 coated CNTs and pristine CNTs. The TG-DTA curve of the CeO_2 coated CNTs in Fig. 7(a) indicates a mass loss with two steps. It is obvious that the first step with the DTA peak around 100 °C is due to the loss of absorbed water from the sample. The second step with the broad peaks ranging from 450 to 630 °C is due to the gradual decomposition of CNT template, which can be confirmed by the test of pristine CNTs shown in Fig. 7(b). It is well known that the decomposition temperature of CNTs varies with the tube diameter and the sites (the tip

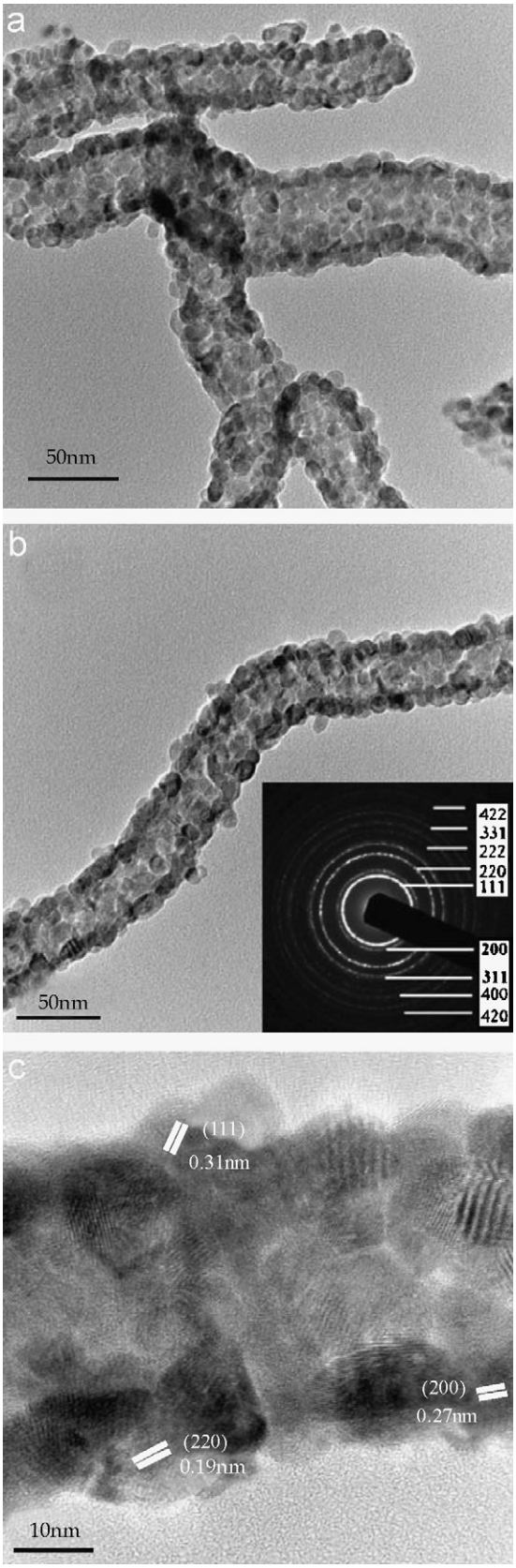

Fig. 2. TEM image: (a) of CeO_2 nanotubes. TEM image (b), SAED pattern (b, inset) and HRTEM image (c) of the single nanotube.

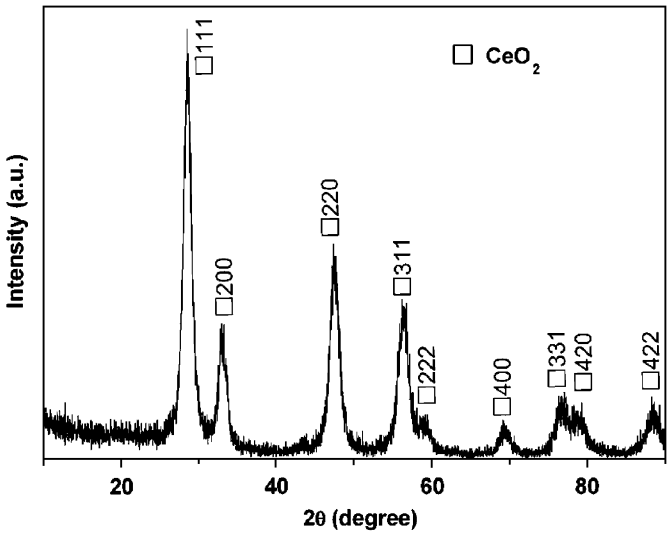

Fig. 3. XRD patterns of CeO_2 nanotubes.

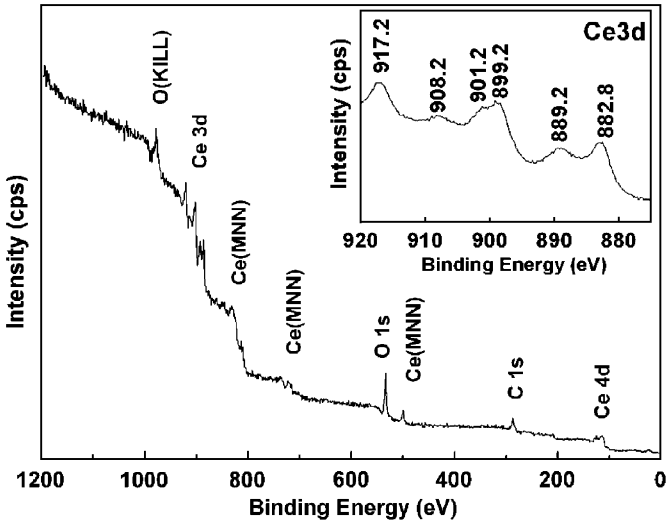

Fig. 4. XPS wide spectrum and Ce 3d spectrum (inset) of CeO_2 nanotubes.

and defective sites have a higher reactivity than that of the other sites [18]), and thus various decomposition temperature indicates the broad peaks. It should be noted that the decomposition temperature of CNT template is lower than that of pristine CNTs due to the high oxidation performance of CeO_2. CNT template cannot be completely removed until 630 °C (Fig. 7(a)), which is higher than the actual calcination temperature (500 °C). It can be explained that the different heating rate and heat preservation time were employed as compared with the actual preparation process.

It is obvious that the formation of CeO_2 coated CNTs is pre-requisite to the formation of CeO_2 nanotubes. In our experiment, the preparation process employed by untreated CNTs was also carried out. Not the uniform composites but the mixtures of the agglomeration of nanoparticles and CNTs were observed in Fig. 8. It can be concluded that the

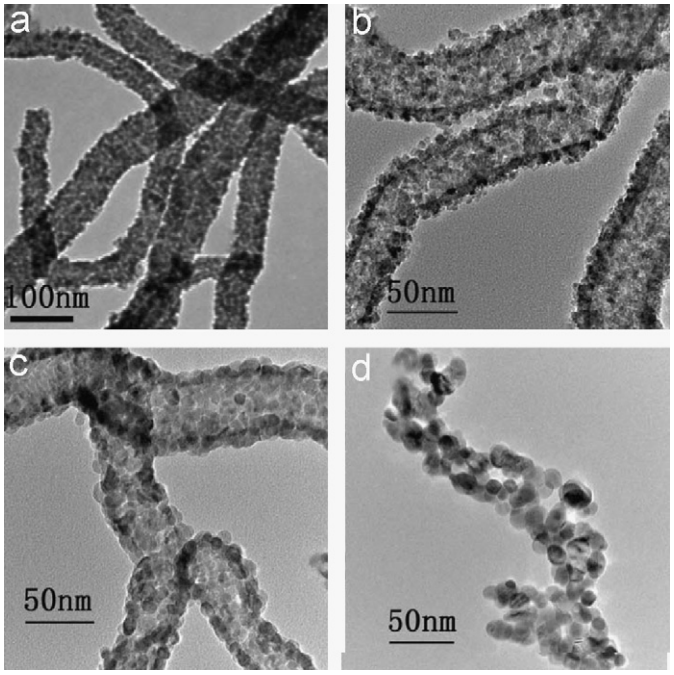

Fig. 5. TEM images of the samples calcined at various temperatures. (a) Uncalcined, (b)calcined at 450 °C, (c)calcined at 500 °C, and (d) calcined at 550 °C.

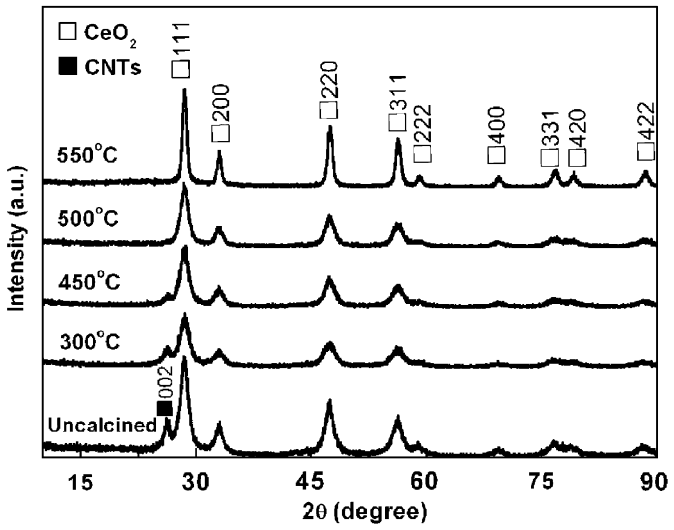

Fig. 6. XRD patterns of the samples calcined at various temperatures.

pretreatment of CNTs plays an important role in the formation of CeO_2 coated CNTs. It can be explained as follows. The zeta potential of the untreated and treated CNTs was measured in Fig. 9. For untreated CNTs, the absolute value of the zeta potential is smaller than 30 mV, and the isoelectric point is around pH = 7, indicating the low surface charge or few acidic groups on untreated CNTs. The present treatment is successful because nitric acid treated CNTs have a higher zeta potential value over a wide pH range (3–12) and the isoelectric point is around pH = 2, indicating the high surface charge or many acidic

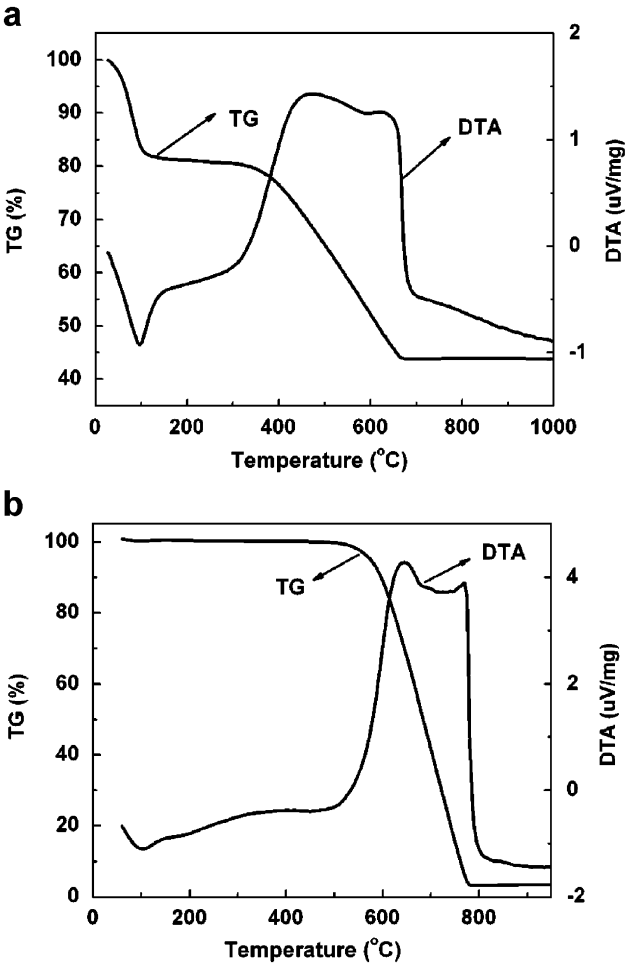

Fig. 7. TG-DTA curves of (a) the CeO_2-coated CNTs and the CeO_2-coated CNTs pristine (b).

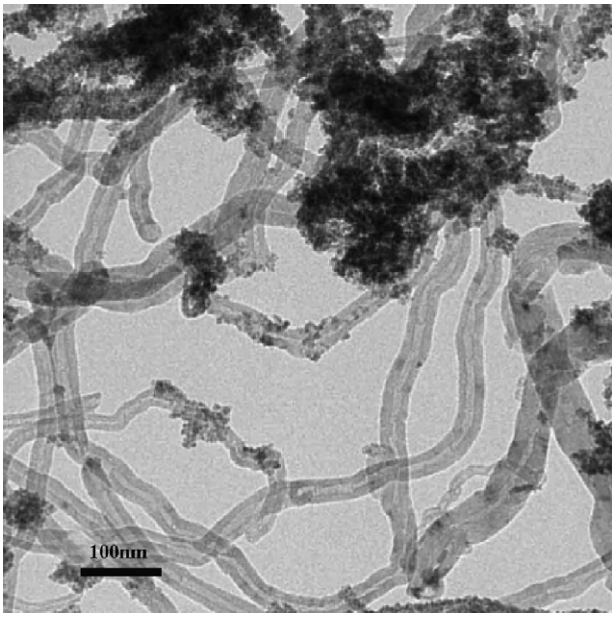

Fig. 8. TEM image of the mixtures of CeO_2 nanoparticles and CNTs.

groups on treated CNTs [19]. The stability of the dispersions is largely determined by the electrostatic repulsion due to the surface charge [19]. It may be seen that the separation of treated CNTs is easily achieved at wide pH values (3–12). It should be noted that the dispersability of treated CNTs is related to the ionization of acidic groups introduced by nitric acid treatment

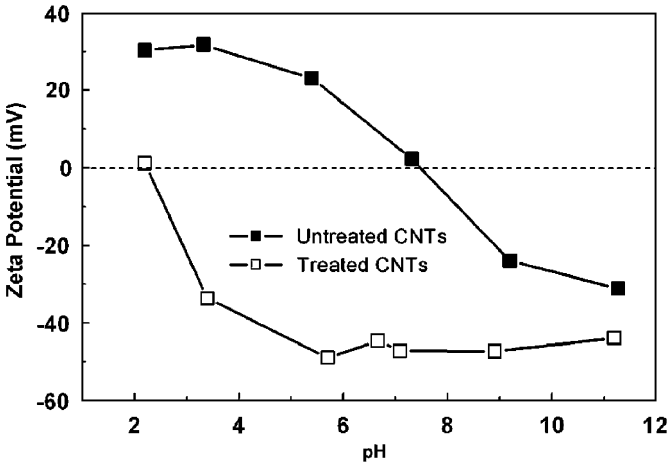

Fig. 9. Zeta potential of untreated and treated CNTs as a function of pH, in aqueous solutions at a concentration of 0.05 mg/mL.

(CNT−COOH = CNT−COO^- + H^+; CNT−OH = CNT−O^- + H^+) and the adsorption of ions such as Ce^{3+} from the aqueous suspension [19]. The high zeta potential can prevent the treated CNTs from aggregating and thereby stabilizes the suspension, which is also in favor of the formation of CeO_2 coated CNTs.

A control experiment was also carried out to investigate the effect of the molar ratio of Ce^{3+} to CNTs. Fig. 10 shows that the molar ratio (0.4–12) can slightly affect the morphologies of CeO_2 coated CNTs. When the molar ratio is low, a few tiny CeO_2 nanoparticles firstly deposit on the surface active sites of CNTs and some parts of CNTs are still naked (Fig. 10(a)). With the increase of the molar ratio, the CNTs are uniformly coated by a layer of tiny nanoparticles (Figs. 10(b)–(d)). Finally, some nanoparticles agglomerate and are nearly separate from the coating layers when the molar ratio is extremely high, which can be confirmed by TEM shown in Fig. 10(e).

According to the above analysis, the formation mechanism of CeO_2 nanotubes may be suggested in Scheme 1. CNTs are first treated by nitric acid, and then the surface acidic groups on the nanotubes can adsorb Ce^{3+} and form metal-oxygen bonds [20]. With addition of NaOH solution, CeO_2 nanoparticles are in-situ deposited resulting in the formation of CeO_2 coated CNTs. It is noted that the Ce

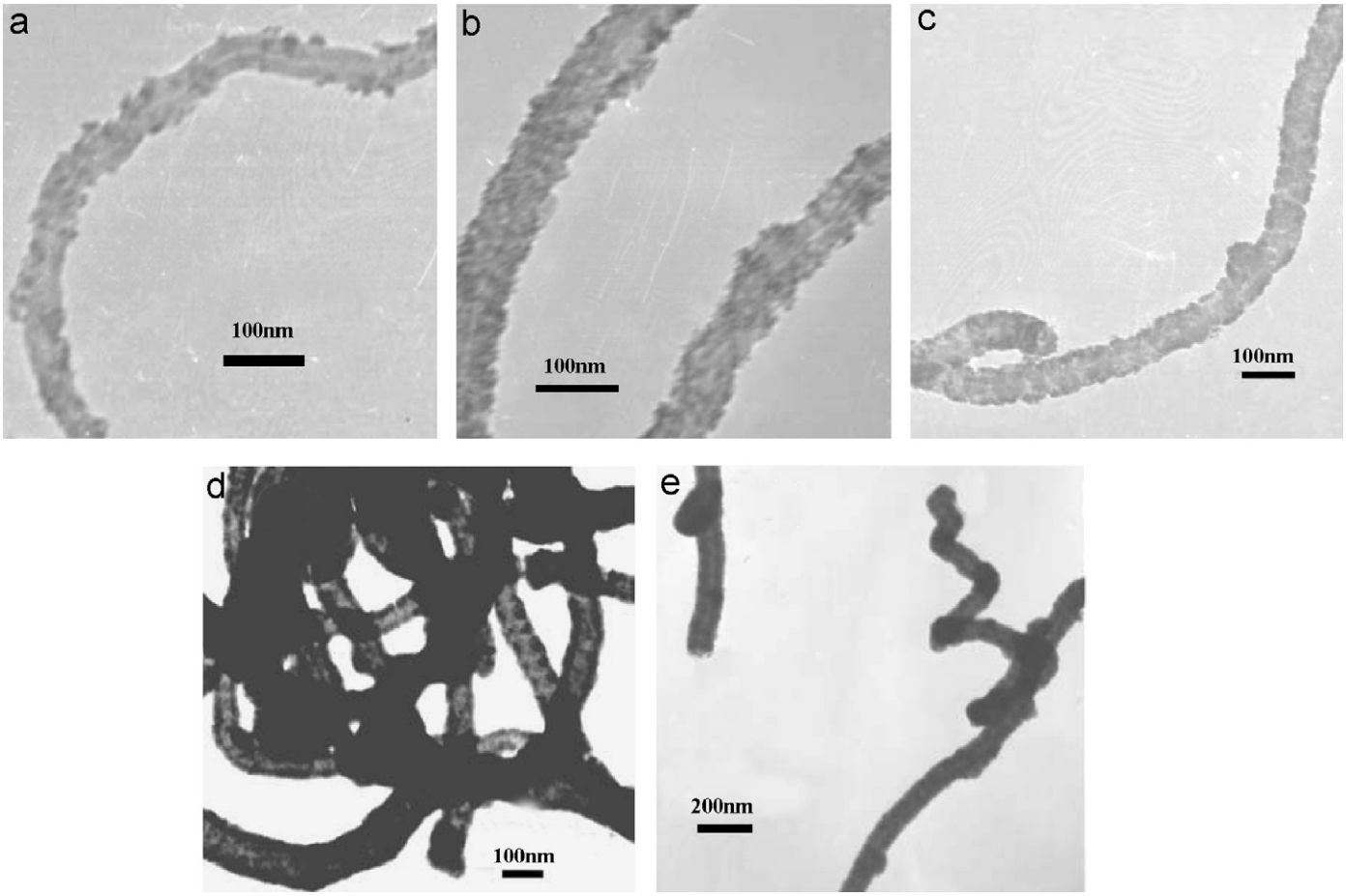

Fig. 10. TEM images of the samples prepared with various molar ratios of Ce^{3+} to CNTs. (a) 0.4, (b) 0.8, (c) 1.2, (d) 6, and (e) 12.

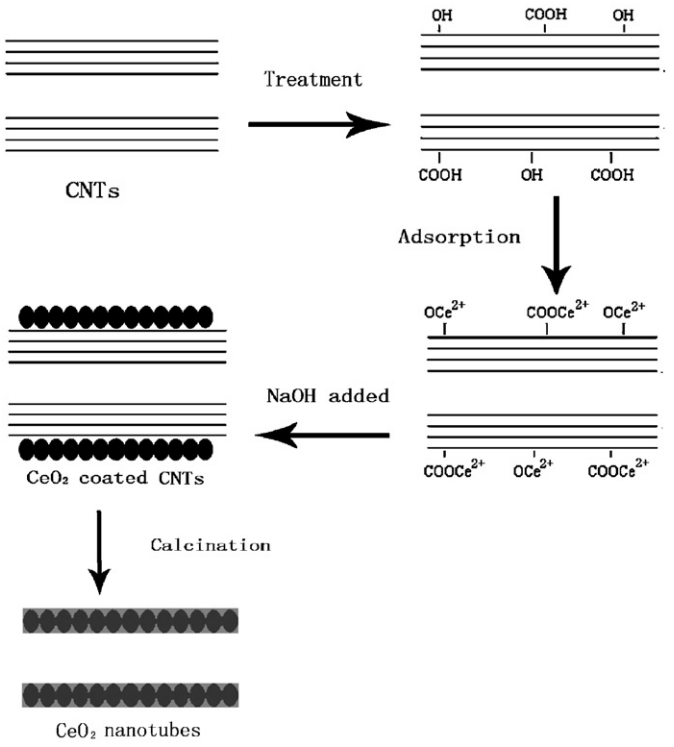

Scheme 1. The formation mechanism of CeO_2 nanotubes.

(III) oxidation state is very unstable as compared with the Ce (IV) oxidation state especially in alkaline solution and in the presence of air [17,21], due to the low reduction potential of Ce(IV)–Ce(III) [22], and thus the intermediate products, such as $Ce(OH)_3$, are hard to exist. The previous reports [17,21] show the direct synthesis process of CeO_2 as follows:

$$4Ce^{3+} + 12OH^- + O_2 + (4n-6)H_2O \rightarrow 4(CeO_2 \cdot nH_2O)$$

$$CeO_2 \cdot nH_2O \rightarrow CeO_2 + nH_2O.$$

Our XRD measurements of the uncalcined sample (Fig. 6) confirm that CeO_2 forms directly without observation of any other cerium compound. After calcining CeO_2/CNT composites at a suitable temperature, CeO_2 nanotubes are obtained by removing CNT templates.

4. Conclusions

In summary, for the first time, CeO_2 nanotubes have been synthesized using CNTs as templates by a liquid phase deposition method. It is found that the CeO_2 nanotubes with a polycrystalline face-centered cubic phase are composed of many tiny interconnected grains at various orientations (average grain size of 10 nm). The pretreatment of CNTs and calcination temperature were confirmed to be the crucial factors determining the formation of CeO_2 nanotubes. Such nanotubes are very interesting for further studies on their physical and chemical properties. Considering the convenience of the procedure, this CNT template-assisted route is promising and may be extended to fabricate other metal oxide nanotubes.

Acknowledgments

The authors acknowledge the support of Nano Science and Techology Special Project of Shanghai, China (0452nm027).

References

[1] S. Iijima, Nature 354 (1991) 56.
[2] P.M. Ajayan, Chem. Rev. 99 (1999) 1787.
[3] H. Yu, Z. Zhang, M. Han, X. Hao, F. Zhu, J. Am. Chem. Soc. 127 (2005) 2378.
[4] G. Malandrino, S.T. Finocchiaro, R. Lo-Nigro, C. Bongiorno, C. Spinella, I.L. Fragala, Chem. Mater. 16 (2004) 5559.
[5] D. Zheng, S. Sun, W. Fan, H. Yu, C. Fan, G. Cao, Z. Yin, X. Song, J. Phys. Chem. B 109 (2005) 16439.
[6] L. Qian, Z.S. Jin, S.Y. Yang, Z.L. Du, X.R. Xu, Chem. Mater. 17 (2005) 5334.
[7] J.S. Lee, S.K. Sim, K.H. Kim, K. Cho, S. Kim, Mater. Sci. Eng. B 122 (2005) 85.
[8] H. Ogihara, S. Takenaka, I. Yamanaka, E. Tanabe, A. Genseki, K. Otsuka, Chem. Mater. 18 (2006) 996.
[9] L. Suber, P. Imperatori, G. Ausanio, F. Fabbri, H. Hofmeister, J. Phys. Chem. B 109 (2005) 7103.
[10] Z. Jiang, T. Xie, G.Z. Wang, X.Y. Yuan, C.H. Ye, W.P. Cai, G.W. Meng, G.H. Li, L.D. Zhang, Mater. Lett. 59 (2005) 416.
[11] Z. Sun, H. Yuan, Z. Liu, B. Han, X. Zhang, Adv. Mater. 17 (2005) 2993.
[12] (a) J. Zhang, X. Ju, Z.Y. Wu, T. Liu, T.D. Hu, Y.N. Xie, Chem. Mater. 13 (2001) 4192;
(b) G. Balducci, M.S. Islam, J. Kaspar, P. Fornasiero, M. Graziani, Chem. Mater. 12 (2000) 677;
(c) T. Sayle, C. Parkerb, D.C. Sayle, Chem. Commun. (2004) 2438;
(d) Z. Wang, X. Feng, J. Phys. Chem. B 107 (2003) 13563;
(e) D.G. Shchukin, R.A. Caruso, Chem. Mater. 16 (2004) 2287.
[13] R.J. La, Z.A. Hu, H.L. Li, X.L. Shang, Y.Y. Yang, Mater. Sci. Eng. A 368 (2004) 145.
[14] (a) C.W. Sun, H. Li, Z.X. Wang, L.Q. Chen, X.J. Huang, Chem. Lett. 33 (2004) 662;
(b) A. Vantomme, Z.Y. Yuan, G.H. Du, B.L. Su, Langmuir 21 (2005) 1132.
[15] C.C. Tang, Y. Bando, B.D. Liu, D. Golberg, Adv. Mater. 17 (2005) 3005.
[16] D.S. Zhang, L.Y. Shi, J.H. Fang, X.K. Li, K. Dai, Mater. Lett. 59 (2005) 4044.
[17] P.X. Huang, F. Wu, B.L. Zhu, X.P. Gao, H.Y. Zhu, T.Y. Yan, W.P. Huang, S.H. Wu, D.Y. Song, J. Phys. Chem. B 109 (2005) 19169.
[18] (a) D. Ugarte, Nature 359 (1992) 707;
(b) P. Ajayan, P. Ichihashi, S. Iijima, Chem. Phys. Lett. 202 (1993) 384.
[19] H. Hu, A. Yu, E. Kim, B. Zhao, M.E. Itkis, E. Bekyarova, R.C. Haddon, J. Phys. Chem. B 109 (2005) 11520.
[20] A. Gomathi, S.R.C. Vivekchand, A. Govindaraj, C.N.R. Rao, Adv. Mater. 17 (2005) 2757.
[21] D.S. Zhang, L.Y. Shi, H.X. Fu, J.H. Fang, Carbon 44 (2006) 2853.
[22] (a) T. Miki, T. Ogawa, M. Haneda, N. Kakuta, A. Ueno, S. Tateishi, S. Matsuura, M. Sato, J. Phys. Chem. 94 (1990) 6464;
(b) C. Veríssimo, O.L. Alves, J. Mater. Chem. 13 (2003) 1378.